

Search for the Production of Scalar Bottom Quarks in $p\bar{p}$ Collisions at $\sqrt{s} = 1.96$ TeV

T. Aaltonen,²⁴ J. Adelman,¹⁴ B. Álvarez González^v,¹² S. Amerio^{dd,44} D. Amidei,³⁵ A. Anastassov,³⁹ A. Annovi,²⁰ J. Antos,¹⁵ G. Apollinari,¹⁸ A. Apresyan,⁴⁹ T. Arisawa,⁵⁸ A. Artikov,¹⁶ J. Asaadi,⁵⁴ W. Ashmanskas,¹⁸ A. Attal,⁴ A. Aurisano,⁵⁴ F. Azfar,⁴³ W. Badgett,¹⁸ A. Barbaro-Galtieri,²⁹ V.E. Barnes,⁴⁹ B.A. Barnett,²⁶ P. Barria^{ff},⁴⁷ P. Bartos,¹⁵ G. Bauer,³³ P.-H. Beauchemin,³⁴ F. Bedeschi,⁴⁷ D. Beecher,³¹ S. Behari,²⁶ G. Bellettini^{ee},⁴⁷ J. Bellinger,⁶⁰ D. Benjamin,¹⁷ A. Beretvas,¹⁸ A. Bhatti,⁵¹ M. Binkley,¹⁸ D. Bisello^{dd,44} I. Bizjak^{jj},³¹ R.E. Blair,² C. Blocker,⁷ B. Blumenfeld,²⁶ A. Bocci,¹⁷ A. Bodek,⁵⁰ V. Boisvert,⁵⁰ D. Bortoletto,⁴⁹ J. Boudreau,⁴⁸ A. Boveia,¹¹ B. Brau^{a,11} A. Bridgeman,²⁵ L. Brigliadori^{cc},⁶ C. Bromberg,³⁶ E. Brubaker,¹⁴ J. Budagov,¹⁶ H.S. Budd,⁵⁰ S. Budd,²⁵ K. Burkett,¹⁸ G. Busetto^{dd,44} P. Bussey,²² A. Buzatu,³⁴ K. L. Byrum,² S. Cabrera^x,¹⁷ C. Calancha,³² S. Camarda,⁴ M. Campanelli,³¹ M. Campbell,³⁵ F. Canelli^{14,18} A. Canepa,⁴⁶ B. Carls,²⁵ D. Carlsmith,⁶⁰ R. Carosi,⁴⁷ S. Carrilloⁿ,¹⁹ S. Carron,¹⁸ B. Casal,¹² M. Casarsa,¹⁸ A. Castro^{cc},⁶ P. Catastini^{ff},⁴⁷ D. Cauz,⁵⁵ V. Cavaliere^{ff},⁴⁷ M. Cavalli-Sforza,⁴ A. Cerri,²⁹ L. Cerrito^q,³¹ S.H. Chang,²⁸ Y.C. Chen,¹ M. Chertok,⁸ G. Chiarelli,⁴⁷ G. Chlachidze,¹⁸ F. Chlebana,¹⁸ K. Cho,²⁸ D. Chokheli,¹⁶ J.P. Chou,²³ K. Chung^o,¹⁸ W.H. Chung,⁶⁰ Y.S. Chung,⁵⁰ T. Chwalek,²⁷ C.I. Ciobanu,⁴⁵ M.A. Ciocci^{ff},⁴⁷ A. Clark,²¹ D. Clark,⁷ G. Compostella,⁴⁴ M.E. Convery,¹⁸ J. Conway,⁸ M. Corbo,⁴⁵ M. Cordelli,²⁰ C.A. Cox,⁸ D.J. Cox,⁸ F. Crescioli^{ee},⁴⁷ C. Cuenca Almenar,⁶¹ J. Cuevas^v,¹² R. Culbertson,¹⁸ J.C. Cully,³⁵ D. Dagenhart,¹⁸ M. Datta,¹⁸ T. Davies,²² P. de Barbaro,⁵⁰ S. De Cecco,⁵² A. Deisher,²⁹ G. De Lorenzo,⁴ M. Dell'Orso^{ee},⁴⁷ C. Deluca,⁴ L. Demortier,⁵¹ J. Deng^f,¹⁷ M. Deninno,⁶ M. d'Errico^{dd,44} A. Di Canto^{ee},⁴⁷ G.P. di Giovanni,⁴⁵ B. Di Ruzza,⁴⁷ J.R. Dittmann,⁵ M. D'Onofrio,⁴ S. Donati^{ee},⁴⁷ P. Dong,¹⁸ T. Dorigo,⁴⁴ S. Dube,⁵³ K. Ebina,⁵⁸ A. Elagin,⁵⁴ R. Erbacher,⁸ D. Errede,²⁵ S. Errede,²⁵ N. Ershaidat^{bb},⁴⁵ R. Eusebi,⁵⁴ H.C. Fang,²⁹ S. Farrington,⁴³ W.T. Fedorko,¹⁴ R.G. Feild,⁶¹ M. Feindt,²⁷ J.P. Fernandez,³² C. Ferrazza^{gg},⁴⁷ R. Field,¹⁹ G. Flanagan^s,⁴⁹ R. Forrest,⁸ M.J. Frank,⁵ M. Franklin,²³ J.C. Freeman,¹⁸ I. Furic,¹⁹ M. Gallinaro,⁵¹ J. Galyardt,¹³ F. Garbersen,¹¹ J.E. Garcia,²¹ A.F. Garfinkel,⁴⁹ P. Garosi^{ff},⁴⁷ H. Gerberich,²⁵ D. Gerdes,³⁵ A. Gessler,²⁷ S. Giagu^{hh},⁵² V. Giakoumopoulou,³ P. Giannetti,⁴⁷ K. Gibson,⁴⁸ J.L. Gimmell,⁵⁰ C.M. Ginsburg,¹⁸ N. Giokaris,³ M. Giordaniⁱⁱ,⁵⁵ P. Giromini,²⁰ M. Giunta,⁴⁷ G. Giurgiu,²⁶ V. Glagolev,¹⁶ D. Glenzinski,¹⁸ M. Gold,³⁸ N. Goldschmidt,¹⁹ A. Golossanov,¹⁸ G. Gomez,¹² G. Gomez-Ceballos,³³ M. Goncharov,³³ O. González,³² I. Gorelov,³⁸ A.T. Goshaw,¹⁷ K. Goulianos,⁵¹ A. Gresele^{dd,44} S. Grinstein,⁴ C. Grosso-Pilcher,¹⁴ R.C. Group,¹⁸ U. Grundler,²⁵ J. Guimaraes da Costa,²³ Z. Gunay-Unalan,³⁶ C. Haber,²⁹ S.R. Hahn,¹⁸ E. Halkiadakis,⁵³ B.-Y. Han,⁵⁰ J.Y. Han,⁵⁰ F. Happacher,²⁰ K. Hara,⁵⁶ D. Hare,⁵³ M. Hare,⁵⁷ R.F. Harr,⁵⁹ M. Hartz,⁴⁸ K. Hatakeyama,⁵ C. Hays,⁴³ M. Heck,²⁷ J. Heinrich,⁴⁶ M. Herndon,⁶⁰ J. Heuser,²⁷ S. Hewamanage,⁵ D. Hidas,⁵³ C.S. Hill^c,¹¹ D. Hirschbuehl,²⁷ A. Hocker,¹⁸ S. Hou,¹ M. Houlden,³⁰ S.-C. Hsu,²⁹ R.E. Hughes,⁴⁰ M. Hurwitz,¹⁴ U. Husemann,⁶¹ M. Hussein,³⁶ J. Huston,³⁶ J. Incandela,¹¹ G. Introzzi,⁴⁷ M. Iori^{hh},⁵² A. Ivanov^p,⁸ E. James,¹⁸ D. Jang,¹³ B. Jayatilaka,¹⁷ E.J. Jeon,²⁸ M.K. Jha,⁶ S. Jindariani,¹⁸ W. Johnson,⁸ M. Jones,⁴⁹ K.K. Joo,²⁸ S.Y. Jun,¹³ J.E. Jung,²⁸ T.R. Junk,¹⁸ T. Kamon,⁵⁴ D. Kar,¹⁹ P.E. Karchin,⁵⁹ Y. Kato^m,⁴² R. Kephart,¹⁸ W. Ketchum,¹⁴ J. Keung,⁴⁶ V. Khotilovich,⁵⁴ B. Kilminster,¹⁸ D.H. Kim,²⁸ H.S. Kim,²⁸ H.W. Kim,²⁸ J.E. Kim,²⁸ M.J. Kim,²⁰ S.B. Kim,²⁸ S.H. Kim,⁵⁶ Y.K. Kim,¹⁴ N. Kimura,⁵⁸ L. Kirsch,⁷ S. Klimenko,¹⁹ K. Kondo,⁵⁸ D.J. Kong,²⁸ J. Konigsberg,¹⁹ A. Korytov,¹⁹ A.V. Kotwal,¹⁷ M. Kreps,²⁷ J. Kroll,⁴⁶ D. Krop,¹⁴ N. Krumnack,⁵ M. Kruse,¹⁷ V. Krutelyov,¹¹ T. Kuhr,²⁷ N.P. Kulkarni,⁵⁹ M. Kurata,⁵⁶ S. Kwang,¹⁴ A.T. Laasanen,⁴⁹ S. Lami,⁴⁷ S. Lammel,¹⁸ M. Lancaster,³¹ R.L. Lander,⁸ K. Lannon^u,⁴⁰ A. Lath,⁵³ G. Latino^{ff},⁴⁷ I. Lazzizzera^{dd,44} T. LeCompte,² E. Lee,⁵⁴ H.S. Lee,¹⁴ J.S. Lee,²⁸ S.W. Lee^w,⁵⁴ S. Leone,⁴⁷ J.D. Lewis,¹⁸ C.-J. Lin,²⁹ J. Linacre,⁴³ M. Lindgren,¹⁸ E. Lipeles,⁴⁶ A. Lister,²¹ D.O. Litvintsev,¹⁸ C. Liu,⁴⁸ T. Liu,¹⁸ N.S. Lockyer,⁴⁶ A. Loginov,⁶¹ L. Lovas,¹⁵ D. Lucchesi^{dd,44} J. Lueck,²⁷ P. Lujan,²⁹ P. Lukens,¹⁸ G. Lungu,⁵¹ J. Lys,²⁹ R. Lysak,¹⁵ D. MacQueen,³⁴ R. Madrak,¹⁸ K. Maeshima,¹⁸ K. Makhoul,³³ P. Maksimovic,²⁶ S. Malde,⁴³ S. Malik,³¹ G. Manca^e,³⁰ A. Manousakis-Katsikakis,³ F. Margaroli,⁴⁹ C. Marino,²⁷ C.P. Marino,²⁵ A. Martin,⁶¹ V. Martin^k,²² M. Martínez,⁴ R. Martínez-Ballarín,³² P. Mastrandrea,⁵² M. Mathis,²⁶ M.E. Mattson,⁵⁹ P. Mazzanti,⁶ K.S. McFarland,⁵⁰ P. McIntyre,⁵⁴ R. McNulty^j,³⁰ A. Mehta,³⁰ P. Mehtala,²⁴ A. Menzione,⁴⁷ C. Mesropian,⁵¹ T. Miao,¹⁸ D. Mietlicki,³⁵ N. Miladinovic,⁷ R. Miller,³⁶ C. Mills,²³ M. Milnik,²⁷ A. Mitra,¹ G. Mitselmakher,¹⁹ H. Miyake,⁵⁶ S. Moed,²³ N. Moggi,⁶ M.N. Mondragonⁿ,¹⁸ C.S. Moon,²⁸ R. Moore,¹⁸ M.J. Morello,⁴⁷ J. Morlock,²⁷ P. Movilla Fernandez,¹⁸ J. Mülmenstädt,²⁹ A. Mukherjee,¹⁸ Th. Muller,²⁷ P. Murat,¹⁸ M. Mussini^{cc},⁶ J. Nachtman^o,¹⁸ Y. Nagai,⁵⁶ J. Naganoma,⁵⁶ K. Nakamura,⁵⁶ I. Nakano,⁴¹ A. Napier,⁵⁷ J. Nett,⁶⁰ C. Neu^z,⁴⁶ M.S. Neubauer,²⁵ S. Neubauer,²⁷ J. Nielsen^g,²⁹ L. Nodulman,² M. Norman,¹⁰ O. Norniella,²⁵ E. Nurse,³¹ L. Oakes,⁴³ S.H. Oh,¹⁷ Y.D. Oh,²⁸ I. Oksuzian,¹⁹ T. Okusawa,⁴² R. Orava,²⁴ K. Osterberg,²⁴ S. Pagan Griso^{dd,44}

C. Pagliarone,⁵⁵ E. Palencia,¹⁸ V. Papadimitriou,¹⁸ A. Papaikonomou,²⁷ A.A. Paramanov,² B. Parks,⁴⁰ S. Pashapour,³⁴ J. Patrick,¹⁸ G. Paulettaⁱⁱ,⁵⁵ M. Paulini,¹³ C. Paus,³³ T. Peiffer,²⁷ D.E. Pellett,⁸ A. Penzo,⁵⁵ T.J. Phillips,¹⁷ G. Piacentino,⁴⁷ E. Pianori,⁴⁶ L. Pinera,¹⁹ K. Pitts,²⁵ C. Plager,⁹ L. Pondrom,⁶⁰ K. Potamianos,⁴⁹ O. Poukhov^{*},¹⁶ F. Prokoshin^y,¹⁶ A. Pronko,¹⁸ F. Ptohosⁱ,¹⁸ E. Pueschel,¹³ G. Punzi^{ee},⁴⁷ J. Pursley,⁶⁰ J. Rademacker^c,⁴³ A. Rahaman,⁴⁸ V. Ramakrishnan,⁶⁰ N. Ranjan,⁴⁹ I. Redondo,³² P. Renton,⁴³ M. Renz,²⁷ M. Rescigno,⁵² S. Richter,²⁷ F. Rimondi^{cc},⁶ L. Ristori,⁴⁷ A. Robson,²² T. Rodrigo,¹² T. Rodriguez,⁴⁶ E. Rogers,²⁵ S. Rolli,⁵⁷ R. Roser,¹⁸ M. Rossi,⁵⁵ R. Rossin,¹¹ P. Roy,³⁴ A. Ruiz,¹² J. Russ,¹³ V. Rusu,¹⁸ B. Rutherford,¹⁸ H. Saarikko,²⁴ A. Safonov,⁵⁴ W.K. Sakumoto,⁵⁰ L. Santiⁱⁱ,⁵⁵ L. Sartori,⁴⁷ K. Sato,⁵⁶ A. Savoy-Navarro,⁴⁵ P. Schlabach,¹⁸ A. Schmidt,²⁷ E.E. Schmidt,¹⁸ M.A. Schmidt,¹⁴ M.P. Schmidt^{*},⁶¹ M. Schmitt,³⁹ T. Schwarz,⁸ L. Scodellaro,¹² A. Scribano^{ff},⁴⁷ F. Scuri,⁴⁷ A. Sedov,⁴⁹ S. Seidel,³⁸ Y. Seiya,⁴² A. Semenov,¹⁶ L. Sexton-Kennedy,¹⁸ F. Sforza^{ee},⁴⁷ A. Sfyrta,²⁵ S.Z. Shalhout,⁵⁹ T. Shears,³⁰ P.F. Shepard,⁴⁸ M. Shimojima^t,⁵⁶ S. Shiraishi,¹⁴ M. Shochet,¹⁴ Y. Shon,⁶⁰ I. Shreyber,³⁷ A. Simonenko,¹⁶ P. Sinervo,³⁴ A. Sisakyan,¹⁶ A.J. Slaughter,¹⁸ J. Slaunwhite,⁴⁰ K. Sliwa,⁵⁷ J.R. Smith,⁸ F.D. Snider,¹⁸ R. Snihur,³⁴ A. Soha,¹⁸ S. Somalwar,⁵³ V. Sorin,⁴ P. Squillacioti^{ff},⁴⁷ M. Stanitzki,⁶¹ R. St. Denis,²² B. Stelzer,³⁴ O. Stelzer-Chilton,³⁴ D. Stentz,³⁹ J. Strologas,³⁸ G.L. Strycker,³⁵ J.S. Suh,²⁸ A. Sukhanov,¹⁹ I. Suslov,¹⁶ A. Taffard^f,²⁵ R. Takashima,⁴¹ Y. Takeuchi,⁵⁶ R. Tanaka,⁴¹ J. Tang,¹⁴ M. Tecchio,³⁵ P.K. Teng,¹ J. Thom^h,¹⁸ J. Thome,¹³ G.A. Thompson,²⁵ E. Thomson,⁴⁶ P. Tipton,⁶¹ P. Ttito-Guzmán,³² S. Tkaczyk,¹⁸ D. Toback,⁵⁴ S. Tokar,¹⁵ K. Tollefson,³⁶ T. Tomura,⁵⁶ D. Tonelli,¹⁸ S. Torre,²⁰ D. Torretta,¹⁸ P. Totaroⁱⁱ,⁵⁵ S. Tourneur,⁴⁵ M. Trovato^{gg},⁴⁷ S.-Y. Tsai,¹ Y. Tu,⁴⁶ N. Turini^{ff},⁴⁷ F. Ukegawa,⁵⁶ S. Uozumi,²⁸ N. van Remortel^b,²⁴ A. Varganov,³⁵ E. Vataga^{gg},⁴⁷ F. Vázquezⁿ,¹⁹ G. Velev,¹⁸ C. Vellidis,³ M. Vidal,³² I. Vila,¹² R. Vilar,¹² M. Vogel,³⁸ I. Volobouev^w,²⁹ G. Volpi^{ee},⁴⁷ P. Wagner,⁴⁶ R.G. Wagner,² R.L. Wagner,¹⁸ W. Wagner^{aa},²⁷ J. Wagner-Kuhr,²⁷ T. Wakisaka,⁴² R. Wallny,⁹ S.M. Wang,¹ A. Warburton,³⁴ D. Waters,³¹ M. Weinberger,⁵⁴ J. Weinelt,²⁷ W.C. Wester III,¹⁸ B. Whitehouse,⁵⁷ D. Whiteson^f,⁴⁶ A.B. Wicklund,² E. Wicklund,¹⁸ S. Wilbur,¹⁴ G. Williams,³⁴ H.H. Williams,⁴⁶ P. Wilson,¹⁸ B.L. Winer,⁴⁰ P. Wittich^h,¹⁸ S. Wolbers,¹⁸ C. Wolfe,¹⁴ H. Wolfe,⁴⁰ T. Wright,³⁵ X. Wu,²¹ F. Würthwein,¹⁰ A. Yagil,¹⁰ K. Yamamoto,⁴² J. Yamaoka,¹⁷ U.K. Yang^r,¹⁴ Y.C. Yang,²⁸ W.M. Yao,²⁹ G.P. Yeh,¹⁸ K. Yi^o,¹⁸ J. Yoh,¹⁸ K. Yorita,⁵⁸ T. Yoshida^l,⁴² G.B. Yu,¹⁷ I. Yu,²⁸ S.S. Yu,¹⁸ J.C. Yun,¹⁸ A. Zanetti,⁵⁵ Y. Zeng,¹⁷ X. Zhang,²⁵ Y. Zheng^d,⁹ and S. Zucchelli^{cc6}

(CDF Collaboration[†])

¹*Institute of Physics, Academia Sinica, Taipei, Taiwan 11529, Republic of China*

²*Argonne National Laboratory, Argonne, Illinois 60439*

³*University of Athens, 157 71 Athens, Greece*

⁴*Institut de Física d'Altes Energies, Universitat Autònoma de Barcelona, E-08193, Bellaterra (Barcelona), Spain*

⁵*Baylor University, Waco, Texas 76798*

⁶*Istituto Nazionale di Fisica Nucleare Bologna, ^{cc}University of Bologna, I-40127 Bologna, Italy*

⁷*Brandeis University, Waltham, Massachusetts 02254*

⁸*University of California, Davis, Davis, California 95616*

⁹*University of California, Los Angeles, Los Angeles, California 90024*

¹⁰*University of California, San Diego, La Jolla, California 92093*

¹¹*University of California, Santa Barbara, Santa Barbara, California 93106*

¹²*Instituto de Física de Cantabria, CSIC-University of Cantabria, 39005 Santander, Spain*

¹³*Carnegie Mellon University, Pittsburgh, PA 15213*

¹⁴*Enrico Fermi Institute, University of Chicago, Chicago, Illinois 60637*

¹⁵*Comenius University, 842 48 Bratislava, Slovakia; Institute of Experimental Physics, 040 01 Kosice, Slovakia*

¹⁶*Joint Institute for Nuclear Research, RU-141980 Dubna, Russia*

¹⁷*Duke University, Durham, North Carolina 27708*

¹⁸*Fermi National Accelerator Laboratory, Batavia, Illinois 60510*

¹⁹*University of Florida, Gainesville, Florida 32611*

²⁰*Laboratori Nazionali di Frascati, Istituto Nazionale di Fisica Nucleare, I-00044 Frascati, Italy*

²¹*University of Geneva, CH-1211 Geneva 4, Switzerland*

²²*Glasgow University, Glasgow G12 8QQ, United Kingdom*

²³*Harvard University, Cambridge, Massachusetts 02138*

²⁴*Division of High Energy Physics, Department of Physics, University of Helsinki and Helsinki Institute of Physics, FIN-00014, Helsinki, Finland*

²⁵*University of Illinois, Urbana, Illinois 61801*

²⁶*The Johns Hopkins University, Baltimore, Maryland 21218*

²⁷*Institut für Experimentelle Kernphysik, Karlsruhe Institute of Technology, D-76131 Karlsruhe, Germany*

²⁸*Center for High Energy Physics: Kyungpook National University, Daegu 702-701, Korea; Seoul National University, Seoul 151-742,*

- Korea; Sungkyunkwan University, Suwon 440-746,
 Korea; Korea Institute of Science and Technology Information,
 Daejeon 305-806, Korea; Chonnam National University, Gwangju 500-757,
 Korea; Chonbuk National University, Jeonju 561-756, Korea
²⁹Ernest Orlando Lawrence Berkeley National Laboratory, Berkeley, California 94720
³⁰University of Liverpool, Liverpool L69 7ZE, United Kingdom
³¹University College London, London WC1E 6BT, United Kingdom
³²Centro de Investigaciones Energeticas Medioambientales y Tecnologicas, E-28040 Madrid, Spain
³³Massachusetts Institute of Technology, Cambridge, Massachusetts 02139
³⁴Institute of Particle Physics: McGill University, Montréal, Québec,
 Canada H3A 2T8; Simon Fraser University, Burnaby, British Columbia,
 Canada V5A 1S6; University of Toronto, Toronto, Ontario,
 Canada M5S 1A7; and TRIUMF, Vancouver, British Columbia, Canada V6T 2A3
³⁵University of Michigan, Ann Arbor, Michigan 48109
³⁶Michigan State University, East Lansing, Michigan 48824
³⁷Institution for Theoretical and Experimental Physics, ITEP, Moscow 117259, Russia
³⁸University of New Mexico, Albuquerque, New Mexico 87131
³⁹Northwestern University, Evanston, Illinois 60208
⁴⁰The Ohio State University, Columbus, Ohio 43210
⁴¹Okayama University, Okayama 700-8530, Japan
⁴²Osaka City University, Osaka 588, Japan
⁴³University of Oxford, Oxford OX1 3RH, United Kingdom
⁴⁴Istituto Nazionale di Fisica Nucleare, Sezione di Padova-Trento, ^{dd}University of Padova, I-35131 Padova, Italy
⁴⁵LPNHE, Universite Pierre et Marie Curie/IN2P3-CNRS, UMR7585, Paris, F-75252 France
⁴⁶University of Pennsylvania, Philadelphia, Pennsylvania 19104
⁴⁷Istituto Nazionale di Fisica Nucleare Pisa, ^{ee}University of Pisa,
^{ff}University of Siena and ^{gg}Scuola Normale Superiore, I-56127 Pisa, Italy
⁴⁸University of Pittsburgh, Pittsburgh, Pennsylvania 15260
⁴⁹Purdue University, West Lafayette, Indiana 47907
⁵⁰University of Rochester, Rochester, New York 14627
⁵¹The Rockefeller University, New York, New York 10021
⁵²Istituto Nazionale di Fisica Nucleare, Sezione di Roma 1,
^{hh}Sapienza Università di Roma, I-00185 Roma, Italy
⁵³Rutgers University, Piscataway, New Jersey 08855
⁵⁴Texas A&M University, College Station, Texas 77843
⁵⁵Istituto Nazionale di Fisica Nucleare Trieste/Udine,
 I-34100 Trieste, ⁱⁱUniversity of Trieste/Udine, I-33100 Udine, Italy
⁵⁶University of Tsukuba, Tsukuba, Ibaraki 305, Japan
⁵⁷Tufts University, Medford, Massachusetts 02155
⁵⁸Waseda University, Tokyo 169, Japan
⁵⁹Wayne State University, Detroit, Michigan 48201
⁶⁰University of Wisconsin, Madison, Wisconsin 53706
⁶¹Yale University, New Haven, Connecticut 06520
 (Dated: December 1, 2017)

We report on a search for direct scalar bottom quark (sbottom) pair production in $p\bar{p}$ collisions at $\sqrt{s} = 1.96$ TeV, in events with large missing transverse energy and two jets of hadrons in the final state, where at least one of the jets is required to be identified as originating from a b quark. The study uses a CDF Run II data sample corresponding to 2.65 fb^{-1} of integrated luminosity. The data are in agreement with the standard model. In an R-parity conserving minimal supersymmetric scenario, and assuming that the sbottom decays exclusively into a bottom quark and a neutralino, 95% confidence-level upper limits on the sbottom pair production cross section of 0.1 pb are obtained. For neutralino masses below 70 GeV/ c^2 , sbottom masses up to 230 GeV/ c^2 are excluded at 95% confidence level.

PACS numbers: 14.80.Ly, 12.60.Jv

*Deceased

[†]With visitors from ^aUniversity of Massachusetts Amherst, Amherst, Massachusetts 01003, ^bUniversiteit Antwerpen, B-2610

Antwerp, Belgium, ^cUniversity of Bristol, Bristol BS8 1TL, United Kingdom, ^dChinese Academy of Sciences, Beijing 100864, China, ^eIstituto Nazionale di Fisica Nucleare, Sezione di Cagliari,

Supersymmetry (SUSY) [1] is an extension of the standard model (SM) that naturally solves the hierarchy problem [2] and provides a possible candidate for dark matter in the Universe. SUSY doubles the SM spectrum of particles by introducing a new supersymmetric partner (sparticle) for each particle in the SM. In particular, a new scalar field is associated with each left- and right-handed quark state, and two SUSY mass eigenstates \tilde{q}_1 and \tilde{q}_2 result from the mixing of the scalar fields. In some SUSY scenarios, for which the ratio of the vacuum expectation values of the two supersymmetric Higgs fields becomes large, a significant mass difference between eigenstates in the sbottom quark sector can occur, leading to a rather light sbottom \tilde{b}_1 mass state. In a generic minimal supersymmetric extension of the SM (MSSM) and assuming R-parity conservation [1], sparticles are produced in pairs and the lightest supersymmetric particle (LSP) is stable and identified as the neutralino $\tilde{\chi}_1^0$. Assuming a SUSY particle mass hierarchy such that the sbottom decays exclusively as $\tilde{b}_1 \rightarrow b\tilde{\chi}_1^0$, the expected signal for direct sbottom pair production is characterized by the presence of two energetic jets from the hadronization of the bottom quarks and large missing transverse energy \cancel{E}_T [3] from the two LSPs in the final state. Results on searches in this channel using Tevatron data have been previously reported by both the CDF and D0 experiments in Run II [4] [5]. This Letter presents new results based on an almost ten times larger data sample collected by the CDF experiment, corresponding to 2.65 fb^{-1} of integrated luminosity.

The CDF II detector is described in detail elsewhere [6]. The detector has a charged particle tracking system that is immersed in a 1.4 T solenoidal magnetic field coaxial with the beam line, and provides coverage in the pseudorapidity [3] range $|\eta| \leq 2$. Segmented sampling calorimeters, arranged in a projective tower geome-

try, surround the tracking system and measure the energy of interacting particles for $|\eta| < 3.6$. Cherenkov counters in the region $3.7 < |\eta| < 4.7$ measure the number of inelastic $p\bar{p}$ collisions to determine the luminosity [7].

The data are collected using a three-level trigger system that selects events with at least one calorimeter cluster with E_T above 100 GeV. The events are then required to have a primary vertex with a z position within 60 cm of the nominal interaction point. Jets are reconstructed from the energy deposits in the calorimeter towers using a cone-based algorithm [8] with cone radius $R = \sqrt{\Delta\eta^2 + \Delta\phi^2} = 0.4$, and the measured E_T^{jet} is corrected for detector effects and contributions from multiple $p\bar{p}$ interactions per crossing at high instantaneous luminosity, as discussed in Ref. [9]. The events are initially selected with $\cancel{E}_T > 10$ GeV and two jets with corrected transverse energy $E_T^{\text{jet}} > 25$ GeV and pseudorapidity $|\eta^{\text{jet}}| < 2.0$, where at least one of the two jets is required to have $|\eta^{\text{jet}}| < 1.1$. Events with additional jets with $E_T^{\text{jet}} > 15$ GeV and $|\eta^{\text{jet}}| < 2.8$ are rejected. The effect of the trigger selection is studied using control data samples, parametrized as a function of \cancel{E}_T and the transverse energy of the leading jet $E_T^{\text{jet}(1)}$, and consistently taken into account [10]. At a given \cancel{E}_T , the trigger efficiency increases with increasing $E_T^{\text{jet}(1)}$. Finally, at least one of the two leading jets is required to originate from a b -quark jet candidate, using the default CDF b -jet tagging algorithm (SECVTX) [11], based on the presence of a displaced vertex due to the decay of a b hadron inside the jet.

The SM QCD multijet background contribution with large \cancel{E}_T , due to the mismeasurement of the jet energies in the calorimeters, is suppressed by requiring an azimuthal separation $\Delta\phi(\cancel{E}_T - \text{jet}) > 0.4$ for the two jets in the event. The SM background contributions with energetic electrons [12] from W and Z decays and reconstructed as jets in the final state are suppressed by requiring $E_{T,\text{em}}^{\text{jet}}/E_T^{\text{jet}} < 0.9$ for each jet, where $E_{T,\text{em}}^{\text{jet}}$ denotes the electromagnetic component of the jet transverse energy. In addition, events with isolated tracks with transverse momentum $p_{T,\text{track}}$ above 10 GeV/ c are vetoed, thus rejecting backgrounds with W or Z bosons decaying into muons or tau leptons. Beam-related backgrounds and cosmic rays are eliminated by requiring an average jet electromagnetic fraction $f_{\text{em}} > 0.15$ and an average charged particle fraction $f_{\text{ch}} > 0.15$, as defined in [13]. The requirements on f_{em} and f_{ch} reject events with anomalous energy deposition in the hadronic section of the calorimeter or energy deposits in the calorimeter inconsistent with the observed activity in the tracking system, and have no significant effect on SUSY signal and SM background physics samples.

The dominant source of background in the analysis is due to events with a light-flavor jet which is misidentified as a b -jet (mistags). There are also contributions

09042 Monserrato (Cagliari), Italy, ^fUniversity of California Irvine, Irvine, CA 92697, ^gUniversity of California Santa Cruz, Santa Cruz, CA 95064, ^hCornell University, Ithaca, NY 14853, ⁱUniversity of Cyprus, Nicosia CY-1678, Cyprus, ^jUniversity College Dublin, Dublin 4, Ireland, ^kUniversity of Edinburgh, Edinburgh EH9 3JZ, United Kingdom, ^lUniversity of Fukui, Fukui City, Fukui Prefecture, Japan 910-0017 ^mKinki University, Higashi-Osaka City, Japan 577-8502 ⁿUniversidad Iberoamericana, Mexico D.F., Mexico, ^oUniversity of Iowa, Iowa City, IA 52242, ^pKansas State University, Manhattan, KS 66506 ^qQueen Mary, University of London, London, E1 4NS, England, ^rUniversity of Manchester, Manchester M13 9PL, England, ^sMuons, Inc., Batavia, IL 60510, ^tNagasaki Institute of Applied Science, Nagasaki, Japan, ^uUniversity of Notre Dame, Notre Dame, IN 46556, ^vUniversity de Oviedo, E-33007 Oviedo, Spain, ^wTexas Tech University, Lubbock, TX 79609, ^xIFIC(CSIC-Universitat de Valencia), 56071 Valencia, Spain, ^yUniversidad Tecnica Federico Santa Maria, 110v Valparaiso, Chile, ^zUniversity of Virginia, Charlottesville, VA 22906 ^{aa}Bergische Universität Wuppertal, 42097 Wuppertal, Germany, ^{bb}Yarmouk University, Irbid 211-63, Jordan ^{jj}On leave from J. Stefan Institute, Ljubljana, Slovenia,

from heavy-flavor QCD multijet events with large \cancel{E}_T and passing the $\Delta\phi(\cancel{E}_T - \text{jet})$ requirement discussed above. In both cases, the background estimation is extracted from data using a procedure similar to that described in [11] and [14], where different data-driven multidimensional parameterizations are employed to estimate the probability for a light-flavor jet in each event to be mistagged, and the probability for a heavy-flavor jet in QCD multijet events to pass the CDF b -tag requirements, respectively.

Simulated event samples are used to determine detector acceptance and reconstruction efficiency, estimate the contribution from the rest of the SM backgrounds with heavy-flavor jets in the final state, and compute the number of expected SUSY signal events. Samples of simulated $t\bar{t}$ and diboson (WW , WZ , and ZZ) processes are generated using the PYTHIA 6.216 [15] Monte Carlo generator with Tune A [16], and normalized to next-to-leading order (NLO) predictions [17, 18]. Samples of simulated $Z/\gamma^*(\rightarrow l^+l^-)+\text{jets}$ ($l = e, \mu, \tau$), $Z(\rightarrow \nu\bar{\nu})+\text{jets}$, and $W(\rightarrow l\nu)+\text{jets}$ events with light- and heavy-flavor jets are generated using the ALPGEN 2.1 program [19] interfaced with the parton-shower model from PYTHIA. The normalization of the boson plus jets heavy-flavor samples includes an additional multiplicative factor $k_{HF} = 1.4 \pm 0.4$ which brings the predicted light-to-heavy-flavor relative contributions in agreement with data [11]. The complete $Z/\gamma^*+\text{jets}$ and $W+\text{jets}$ samples are then normalized to the measured Z and W inclusive cross sections [20]. Finally, samples of single top events are produced using the MADEVENT generator [21] and normalized according to NLO predictions [22]. The SUSY samples are generated in the framework of MSSM using PYTHIA. Masses \tilde{b}_1 and $\tilde{\chi}_1^0$ are fixed, and \tilde{b}_1 is only allowed to decay via $\tilde{b}_1 \rightarrow b\tilde{\chi}_1^0$ channel. A total of 106 different samples have been generated with sbottom mass $M_{\tilde{b}_1}$ in the range between 80 GeV/ c^2 and 280 GeV/ c^2 and neutralino mass $M_{\tilde{\chi}_1^0}$ up to 100 GeV/ c^2 . The samples are normalized to NLO predictions, as implemented in PROSPINO2 [23], using CTEQ6.6 [24] parton distribution functions (PDFs) and renormalization and factorization scales set to $M_{\tilde{b}_1}$. The production cross section depends on $M_{\tilde{b}_1}$ and decreases from 50 pb to 0.01 pb as the sbottom mass increases. The Monte Carlo generated events are passed through a full CDF II detector simulation (based on GEANT3 [25] and GFLASH [26]) and reconstructed and analyzed with the same analysis chain as for the data.

An optimization is performed with the aim to maximize the sensitivity to a SUSY signal across the $\tilde{b}_1 - \tilde{\chi}_1^0$ mass plane. For each of the 106 signal samples considered, the procedure maximizes S/\sqrt{B} , where S denotes the number of SUSY events and B is the total SM background. As the difference $\Delta M \equiv M_{\tilde{b}_1} - M_{\tilde{\chi}_1^0}$ increases, the optimal thresholds on \cancel{E}_T , $E_T^{\text{jet}(1)}$, $E_T^{\text{jet}(2)}$

and $\Delta\phi(\cancel{E}_T - \text{jet}(2))$ for the second leading jet, and H_T , defined as $H_T = \sum_i E_T^{\text{jet}(i)}$ ($i=1-2$), increase. The results from the different SUSY samples are combined to define two single sets of thresholds (see Table 1) that maximize the search sensitivity in the widest range of sbottom and neutralino masses at low ΔM ($\Delta M < 90$ GeV/ c^2) and high ΔM ($\Delta M > 90$ GeV/ c^2), respectively. As an example, for $M_{\tilde{\chi}_1^0} = 70$ GeV/ c^2 and $M_{\tilde{b}_1}$ in the range from 150 GeV/ c^2 to 250 GeV/ c^2 , values for S/\sqrt{B} between 10 and 2.5 are obtained, corresponding to SUSY selection efficiencies of 3% to 10%.

Optimal thresholds					
	\cancel{E}_T	$H_T + \cancel{E}_T$	$E_T^{\text{jet}(1)}$	$E_T^{\text{jet}(2)}$	$\Delta\phi(\cancel{E}_T - \text{jet}(2))$
			GeV		radians
low ΔM	60	165	80	25	0.7
high ΔM	80	300	90	40	0.7

TABLE I: Optimized thresholds on \cancel{E}_T , $H_T + \cancel{E}_T$, $E_T^{\text{jet}(1)}$, $E_T^{\text{jet}(2)}$, and $\Delta\phi(\cancel{E}_T - \text{jet}(2))$ for each ΔM region.

A number of control samples in data is considered to test the validity of the SM background predictions. Samples dominated by QCD multijet events or mistags are obtained by reversing the requirements on either \cancel{E}_T or $E_T^{\text{jet}(2)}$, or using a non-overlapping sample selected with looser b -tagging requirements. Control samples dominated by $Z/\gamma^*+\text{jets}$, $W+\text{jets}$, and top-quark processes, with highly energetic leptons in the final state, are obtained after requiring either $E_{T,\text{em}}^{\text{jet}}/E_T^{\text{jet}} > 0.9$ for at least one of the jets, or selecting events with isolated tracks with $p_{T,\text{track}} > 10$ GeV/ c . Agreement is observed between the data and the SM predictions in each of the control samples.

A detailed study of systematic uncertainties was carried out [10]. The uncertainty on the SM background predictions is dominated by the determination of the b -jet mistag rates, which propagates into an uncertainty in the SM prediction between 13% and 11% as ΔM increases. The uncertainty on the k_{HF} value applied to the boson plus jets heavy-flavor samples translates into an 11% uncertainty in the SM predictions. The dependence on the amount of initial-state and final-state radiation in the Monte Carlo generated samples for top, boson plus jets, and diboson contributions introduces a 6% uncertainty on the SM predictions. Other sources of uncertainty on the predicted SM background are: a 3% uncertainty due to the determination of the b -tagging efficiency in the Monte Carlo simulated samples; a 3% uncertainty from the uncertainties on the absolute normalization of the top quark, diboson, W , and Z Monte Carlo generated processes; and a 2.5% uncertainty from the knowledge of the jet energy scale [9]. In addition, uncertainties related to trigger efficiency and the heavy-flavor QCD multijet background contribute less than 1%

to the final uncertainty. The total systematic uncertainty on the SM predictions varies between 19% and 18% as ΔM increases. In the case of the MSSM signal, various sources of uncertainty on the predicted cross sections at NLO, as determined using PROSPINO2, are considered: the uncertainty due to PDFs is computed using the Hessian method [27] and translates into a 12% uncertainty on the absolute predictions; variations of the renormalization and factorization scale by a factor of two change the theoretical cross sections by about 26%. Uncertainties on the amount of initial- and final-state gluon radiation in the MSSM Monte Carlo generated samples introduce a 10% uncertainty on the signal yields. The 3% uncertainty on the absolute jet energy scale translates into a 9% to 14% uncertainty on the MSSM predictions. Other sources of uncertainty include: a 4% uncertainty due to the determination of the b -tagging efficiency, and a 2% to 1% uncertainty due to the uncertainty on the trigger efficiency. The total systematic uncertainty on the MSSM signal yields varies between 30% and 32% as ΔM increases. Finally, an additional 6% uncertainty on the quoted total integrated luminosity is also taken into account in both SM background and SUSY signal predictions.

Figure 1 shows the measured \cancel{E}_T and $H_T + \cancel{E}_T$ distributions compared to the SM predictions after all final selection criteria are applied. For illustrative purposes, the figure indicates the impact of two given MSSM scenarios. The data are in agreement with the SM predictions within uncertainties for each of the two analyses at low and high ΔM . In Table 2, the observed number of events and the SM predictions are presented in each case. A global χ^2 test applied to all data points in Fig. 1, and including correlations between systematic uncertainties, gives a 30% probability for data to be consistent with the SM.

(2.65 fb ⁻¹)	low ΔM	high ΔM
mistags	51.4 \pm 18.2	18.5 \pm 5.5
QCD jets	7.6 \pm 1.9	1.6 \pm 0.2
top	21.2 \pm 3.4	7.8 \pm 1.3
$Z \rightarrow \nu\bar{\nu}$ +jets	27.7 \pm 8.8	10.9 \pm 3.5
$Z/\gamma^* \rightarrow l^+l^-$ +jets	0.5 \pm 0.2	0.11 \pm 0.04
$W \rightarrow l\nu$ +jets	22.3 \pm 7.3	7.3 \pm 2.4
WW, WZ, ZZ	3.1 \pm 0.5	1.4 \pm 0.2
SM prediction	133.8 \pm 26.4	47.6 \pm 8.8
Events in data	139	38

TABLE II: Number of events in data for the two analyses compared to SM predictions, including statistical and systematic uncertainties summed in quadrature.

The results are translated into 95% confidence level (C.L.) upper limits on the cross section for sbottom pair production at given sbottom and neutralino masses, using a Bayesian approach [28] and including statistical and systematic uncertainties. For the latter, correlations between systematic uncertainties on signal efficiencies and

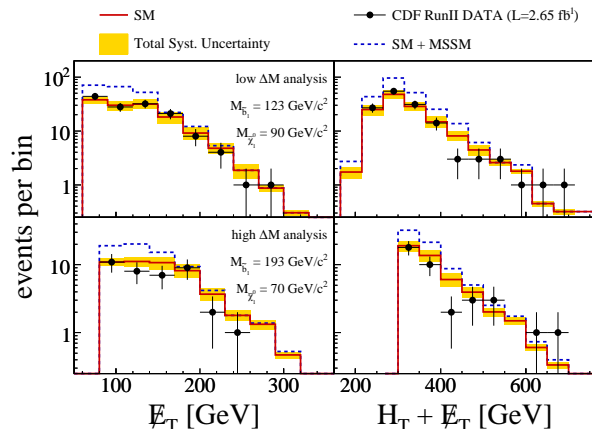


FIG. 1: Measured \cancel{E}_T and $H_T + \cancel{E}_T$ distributions (black dots) for low- ΔM (top) and high- ΔM analyses (bottom), compared to the SM predictions (solid lines) and the SM+MSSM predictions (dashed lines). The shaded bands show the total systematic uncertainty on the SM predictions.

background predictions are taken into account. For each MSSM point considered, observed and expected limits are computed separately for both low- and high- ΔM analyses, and the one with the best expected limit is adopted as the nominal result. Cross sections above 0.1 pb are excluded at 95% C.L. for the range of sbottom masses considered. Similarly, the observed numbers of events in data are translated into 95% C.L. upper limits for sbottom and neutralino masses, for which the uncertainties on the theoretical cross sections are also included in the limit calculation, and where both analyses are combined in the same way as for the cross section limits. Figure 2 shows the expected and observed exclusion regions in the sbottom-neutralino mass plane. For the MSSM scenario considered, sbottom masses up to 230 GeV/ c^2 are excluded at 95% C.L. for neutralino masses below 70 GeV/ c^2 . This analysis extends the previous CDF limits [4] on the sbottom mass by more than 40 GeV/ c^2 .

In summary, we report results on a search for sbottom pair production in $p\bar{p}$ collisions at $\sqrt{s} = 1.96$ TeV, based on 2.65 fb⁻¹ of CDF Run II data. The events are selected with large \cancel{E}_T and two energetic jets in the final state, and at least one jet is required to originate from a b quark. The measurements are in agreement with SM predictions for backgrounds. The results are translated into 95% C.L. upper limits on production cross sections and sbottom and neutralino masses in a given MSSM scenario for which the exclusive decay $\tilde{b}_1 \rightarrow b\tilde{\chi}_1^0$ is assumed, and significantly extend previous CDF results.

We thank the Fermilab staff and the technical staffs of the participating institutions for their vital contributions. This work was supported by the U.S. Department of Energy and National Science Foundation; the Italian Istituto Nazionale di Fisica Nucleare; the Ministry of

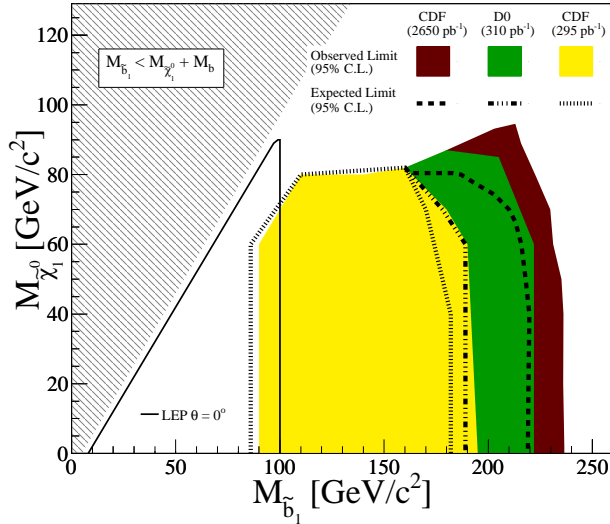


FIG. 2: Exclusion plane at 95 % C.L. as a function of sbottom and neutralino masses. The observed and expected upper limits from this analysis are compared to previous results from CDF and D0 experiments at the Tevatron in Run II [4] [5], and from LEP [29] experiments at CERN with squark mixing angle $\theta = 0^\circ$. The hatched area indicates the kinematically prohibited region in the plane.

Education, Culture, Sports, Science and Technology of Japan; the Natural Sciences and Engineering Research Council of Canada; the National Science Council of the Republic of China; the Swiss National Science Foundation; the A.P. Sloan Foundation; the Bundesministerium für Bildung und Forschung, Germany; the World Class University Program, the National Research Foundation of Korea; the Science and Technology Facilities Council and the Royal Society, UK; the Institut National de Physique Nucleaire et Physique des Particules/CNRS; the Russian Foundation for Basic Research; the Ministerio de Ciencia e Innovación, and Programa Consolider-Ingenio 2010, Spain; the Slovak R&D Agency; and the Academy of Finland.

- [1] H. E. Haber and G. L. Kane, Phys. Rep. **117**, 75 (1985).
 [2] J. Wess and B. Zumino, Phys. Lett. **49B**, 52 (1974).

- [3] CDF uses a cylindrical coordinate system about the beam axis with polar angle θ and azimuthal angle ϕ . We define transverse energy $E_T = E \sin\theta$, transverse momentum $p_T = p \sin\theta$, pseudorapidity $\eta = -\ln(\tan(\frac{\theta}{2}))$, and rapidity $y = \frac{1}{2}\ln(\frac{E+p_z}{E-p_z})$. The missing transverse energy \cancel{E}_T is defined as the norm of $-\sum_i E_T^i \vec{n}_i$, where \vec{n}_i is the component in the azimuthal plane of the unit vector pointing from the interaction point to the i -th calorimeter tower.
- [4] T. Aaltonen *et al.* (CDF Collaboration), Phys. Rev. D **76**, 072010 (2007).
- [5] V.M. Abazov *et al.* (D0 Collaboration), Phys. Rev. Lett. **97**, 171806 (2006).
- [6] D. Acosta *et al.* (CDF Collaboration), Phys. Rev. D **71**, 032001 (2005).
- [7] D. Acosta *et al.*, Nucl. Instrum. Methods A **494**, 57 (2002).
- [8] F. Abe *et al.* (CDF Collaboration), Phys. Rev. D **45**, 1448 (1992).
- [9] A. Bhatti *et al.*, Nucl. Instrum. Methods A **566**, 375 (2006).
- [10] G. De Lorenzo, Ph.D. Thesis, U.A.B., Barcelona (2010).
- [11] D. Acosta *et al.* (CDF Collaboration), Phys. Rev. D **71**, 052003 (2005).
- [12] Charge conjugation is implied throughout the paper.
- [13] T. Aaltonen *et al.* (CDF Collaboration), Phys. Rev. Lett. **102**, 121801 (2009).
- [14] T. Aaltonen *et al.* (CDF Collaboration), Phys. Rev. Lett. **102**, 221801 (2009).
- [15] T. Sjöstrand *et al.*, Comp. Phys. Comm. **135**, 238 (2001).
- [16] T. Affolder *et al.* (CDF Collaboration), Phys. Rev. D **65**, 092002 (2002).
- [17] M. Cacciari *et al.*, J. High Energy Phys. **0404**, 068 (2004).
- [18] J. M. Campbell and R. K. Ellis, Phys. Rev. D **60**, 113006 (1999).
- [19] M.L. Mangano *et al.*, J. High Energy Phys. **07**, 001 (2003).
- [20] A. Abulencia *et al.* (CDF Collaboration), J. Phys. G: Nucl. Part. Phys. **34**, 2457 (2007).
- [21] F. Maltoni and T. Stelzer, J. High Energy Phys. **02**, 027 (2003).
- [22] B. W. Harris *et al.*, Phys. Rev. D **66**, 054024 (2002).
- [23] W. Beenakker *et al.*, Nucl. Phys. B **492**, 51 (1997).
- [24] J. Pumplin *et al.*, J. High Energy Phys. **0207**, 012 (2002).
- [25] R. Brun *et al.*, Tech. Rep. CERN-DD/EE/84-1, (1987).
- [26] G. Grindhammer, M. Rudowicz, and S. Peters, Nucl. Instrum. Methods A **290**, 469 (1990).
- [27] J. Pumplin *et al.*, Phys. Rev. D **65**, 014013 (2001).
- [28] R. Cousins, Am. J. Phys. **63**, 398 (1995).
- [29] LEPSUSYWG/02-06.2, <http://lepsusy.web.cern.ch/lepsusy/>.